Operation of a High-Power Nested Hall Thruster with Reduced Cathode Flow Fraction

Scott J. Hall,* Benjamin A. Jorns,† and Alec D. Gallimore‡
University of Michigan, Ann Arbor, Michigan 48109
and
Dan M. Goebel§
Jet Propulsion Laboratory, California Institute of Technology, Pasadena, California 91109

https://doi.org/10.2514/1.B37929

A high-power nested Hall thruster was operated with cathode flow fractions from 7 to 3% of the total anode flow rate in a two-channel operating configuration at 27 kW total discharge power. The thruster was operated with a state-of-the-art high-current cathode featuring novel external propellant injectors. In stand-alone testing, the cathode has been shown to operate stably up to 300 A with a total flow rate of 36 sccm of xenon. The experiment reported here demonstrated the extensibility of these low flow rates to operation when integrated into the thruster. The impact of the lower-than-nominal flow rates was evaluated using direct thrust measurements, plasma diagnostics, and high-speed current measurement. These results were used to calculate the cathode coupling voltage, most probable beam ion voltage, anode efficiency, total efficiency, and the discharge current oscillation magnitude. It was found that the thruster could be operated with little identifiable change in behavior or performance with a cathode fraction as small as 4%. When the cathode flow fraction was reduced beyond that, the thruster exhibited reduced performance. Implications of these results for future high-power operation of Hall thrusters are discussed.

Nomenclature

I_d	=	discharge current
I_{p2p}	=	peak to peak discharge current oscillations
$\dot{m}_{a,I}$	=	inner channel anode flow rate
$\dot{m}_{a,M}$	=	middle channel anode flow rate
$\dot{m}_{a,O}$	=	outer channel anode flow rate
$\dot{m}_{a,t}$	=	total anode flow rate
$\dot{m}_c$	=	cathode center flow rate
$\dot{m}_{c,t}$	=	total cathode flow rate
$\dot{m}_{\text{inj}}$	=	cathode injector flow rate
$\dot{m}_t$	=	total flow rate
$P_{d,t}$	=	total discharge power
P_{keep}	=	keeper power
P_{mag}	=	magnet power
P_t	=	total power
T	=	thrust
V_{acc}	=	acceleration voltage
V_{avg}	=	average beam ion voltage
V_{cg}	=	cathode-to-ground voltage
Φ_c	=	coupling voltage
$\bar{V}_d$	=	average discharge voltage
$V_{d,I}$	=	inner channel discharge voltage
$V_{d,M}$	=	middle channel discharge voltage
V_p	=	plasma potential
η_a	=	anode efficiency
η_t	=	total efficiency
η_v	=	voltage utilization efficiency

Received 14 December 2019; revision received 7 May 2020; accepted for publication 22 June 2020; published online 10 July 2020.

*Ph.D. Candidate, Department of Aerospace Engineering; currently Research Engineer, Electric Propulsion Systems Branch, HX5, LLC, NASA Glenn Research Center; scott.j.hall@nasa.gov. Member AIAA.

†Assistant Professor, Department of Aerospace Engineering; bjorns@umich.edu. Senior Member AIAA.

‡Robert J. Vlasic Dean of Engineering, Richard F. and Eleanor A. Towner Professor, and Arthur F. Thurnau Professor, Department of Aerospace Engineering; alec.gallimore@umich.edu. Fellow AIAA.

§Senior Research Scientist, Thermal and Propulsion Engineering Section; dan.m.goebel@jpl.nasa.gov. Fellow AIAA.

I. Introduction

TYPICALLY, the cathode flow in Hall thrusters is set as a fraction of the anode flow, often between 7 and 10%, regardless of cathode emitter material [1]. Hall thrusters are usually scaled to high power by maintaining discharge current densities and increasing the exit area and thus the total discharge current [2]. As such, anode flow rates typically scale linearly with thruster power level. The X3, a 100-kW-class, 3-channel nested Hall thruster (NHT), operates with total anode flow rates of approximately 250 mg/s of xenon at its peak discharge current of 250 A [3,4]. By tradition, this would correspond to a cathode flow rates between 17.5 and 25 mg/s. However, previous experience with scaling Hall thrusters to high power suggested that even higher flow fractions might be required. Early NHT operation with a two-channel, 10 kW device suggested that a cathode flow fraction of 10% was necessary for thruster stability [5], and work with a 50 kW single-channel thruster in the early 2000s showed that flow fractions in excess of 30% were needed for thruster stability at certain operating conditions [6].

Complicating the picture further, hollow cathodes do not require the same linear flow rate increase with current to operate properly, and in fact, higher-than-necessary flow rates can disrupt cathode operation. Hollow cathodes typically require internal pressures on the order of 1 Torr to operate effectively and to experience uniform insert heating [7]. With increased internal pressure, the internal or insert plasma of the cathode is pushed downstream, closer to the orifice plate of the cathode, and the region of high plasma density is concentrated, effectively limiting the utilization area of the insert to the downstream end. In the cathode for the NASA Solar electric propulsion Technology Applications Readiness (NSTAR) gridded ion thruster, it was found that the internal pressure caused by the small cathode orifice kept the high-density plasma region constrained to an area less than a centimeter along the insert, using significantly less than the full available area of the insert [8]. By reducing the internal cathode pressure, more of the insert can be used for emission, and the current density required of the emitting area is reduced. This then leads to increased emitter lifetimes.

Thus, the need is apparent to characterize the required cathode flow fraction in the X3 NHT. It appears by the above that the needs of the thruster and its cathode may be at odds, and an important part of

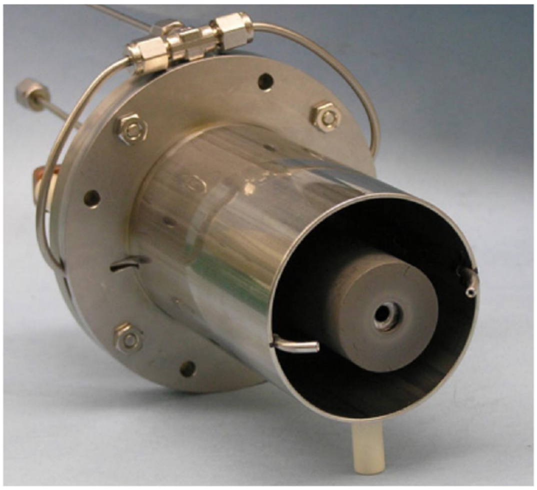

Fig. 1 The high-current LaB_6 hollow cathode with external gas injector tubes located at the 3 and 9 o'clock positions.

the continued development of high-power Hall thrusters, and the high-current cathodes they require, will be to better understand the cathode flow fraction required in this 100 kW, 3-channel NHT. These results have implications not only for optimized operation of this particular thruster, but for high-power Hall thrusters, high-current cathodes, and NHTs more generally.

The X3 NHT is operated with a 300-A-class lanthanum hexaboride (LaB_6) cathode, which has undergone significant development and analysis efforts [7,9] and features a unique design for gas injection external to the cathode tube [9]. The cathode is shown in Fig. 1. These external injectors serve two purposes. First, they provide a secondary flow path for cathode flow in excess of what is necessary to maintain internal pressures on the order of 1 Torr. Second, they reduce energetic ions, a result that has significant implications for cathode lifetimes. Work has shown that this cathode can operate at nominal xenon flow rates of 16 sccm through the cathode and 20 sccm through the injectors up to discharge currents of 250 A when operating in a standalone configuration with a cylindrical anode.

When operating the high-current cathode in the X3 NHT, we specify the cathode flow rate using the total cathode flow fraction (TCFF), which includes both the cathode center and injector flow as

$$\mathrm{TCFF} = \frac{\dot{m}_{c,t}}{\dot{m}_{a,t}} = \frac{\dot{m}_c + \dot{m}_{\mathrm{inj}}}{\dot{m}_{a,I} + \dot{m}_{a,M} + \dot{m}_{a,O}} \tag{1}$$

where $\dot{m}_{c,t}$ is the total cathode flow rate, $\dot{m}_{a,t}$ is the total anode flow rate, $\dot{m}_c$ is the cathode center flow rate, $\dot{m}_{\mathrm{inj}}$ is the flow rate of the cathode external injectors, and the subscripts I, M, and O indicate anode flow rate for the inner, middle, and outer channels, respectively.

The development of this high-current cathode, as well as work done with the H6 6 kW single-channel Hall thruster [1], has suggested that it may be possible to operate the X3 NHT with this cathode at TCFFs much smaller than the traditional 7–10%, especially at high-current conditions. An important first step was performed during early operation of the X3 NHT, which demonstrated that 10% TCFF provided stable operation of the thruster, thus alleviating concerns of required flow fractions as large as the 30% seen in the literature previously [10]. The cathode development effort has clearly shown that the cathode itself is capable of stable high-current operation at relatively low flow rates. However, it has not yet been demonstrated whether this extends to stable operation of the X3 NHT.

Much like the work performed on the H6 reported in [1], we thus seek here to quantify the X3's operation at low cathode flow fractions via thruster stability (as assessed by the magnitude of the discharge current oscillations) and performance (as assessed by thrust, anode and total efficiency, and voltage utilization efficiency). Using thrust values measured directly using the thrust stand described below, anode efficiency is calculated as

$$\eta_a = \frac{T^2}{2\dot{m}_{a,t} P_{d,t}} \tag{2}$$

where T is the measured thrust, $\dot{m}_{a,t}$ is total anode mass flow rate, and $P_{d,t}$ is total discharge power. Both $\dot{m}_{a,t}$ and $P_{d,t}$ are summed across all operating channels. Total efficiency captures the additional losses due to cathode keeper power (if the keeper is drawing current), electromagnet power, and cathode flow rate, and it is thus calculated as

$$\eta_t = \frac{T^2}{2\dot{m}_t P_t} \tag{3}$$

where $\dot{m}_t$ is total mass flow rate,

$$\dot{m}_t = \dot{m}_{a,t} + \dot{m}_{c,t} \tag{4}$$

and P_t is total power,

$$P_t = P_{d,t} + P_{\mathrm{mag}} + P_{\mathrm{keep}} \tag{5}$$

In Eq. (4), $\dot{m}_{c,t}$ is total cathode mass flow rate [as described in Eq. (1)], and in Eq. (5), P_{mag} is power to the electromagnets and P_{keep} is power to the keeper.

Following work performed on the H6, the coupling potential is defined as

$$\phi_c = V_p + |V_{\mathrm{cg}}| \tag{6}$$

where V_p is the downstream plasma potential as measured by a Langmuir probe and V_{cg} is the cathode-to-ground voltage as measured inside the thruster telemetry breakout box. Coupling potential is an inefficiency or loss mechanism in Hall thrusters because it represents the portion of the applied discharge voltage unavailable for ion acceleration.

Another parameter to quantify the voltage inefficiencies is voltage utilization efficiency, which is one of five phenomenological utilization efficiencies typically used for Hall thruster performance analysis [8]. Voltage utilization efficiency in effect describes the fraction of the applied discharge voltage used for ion acceleration; it can be viewed as a description of the efficacy of the conversion of discharge voltage to axial ion velocity. Here, we define voltage utilization efficiency for multichannel operation as

$$\eta_V = \frac{V_{\mathrm{acc}}}{\bar{V}_d} \tag{7}$$

where V_{acc} is the acceleration voltage as calculated from retarding potential analyzer (RPA) measurements as described below, and $\bar{V}_d$ is the average discharge voltage of the operating channels. We define this here for two-channel X3 operation as

$$\bar{V}_d = \frac{V_{d,I} + V_{d,M}}{2} \tag{8}$$

We note that, for all the test conditions described here, the discharge voltages varied between the inner and middle channels by less than 3 V (due simply to the precision with which the power supplies were set), and the averaging of the voltages was essentially a formality.

II. Experimental Apparatus

A. X3 Nested Hall Thruster

The X3 NHT is shown operating inside the vacuum facility at GRC in Fig. 2. The X3 is designed to operate efficiently on both krypton and xenon propellants from 200 to 800 V discharge voltage and at total discharge currents up to 250 A. The total power throttling range of the thruster is 2–200 kW. The thruster is approximately 80 cm in diameter and weighs 230 kg. Each of the three discharge channels features an inner and outer electromagnet for a total of six, each of which is controlled separately.

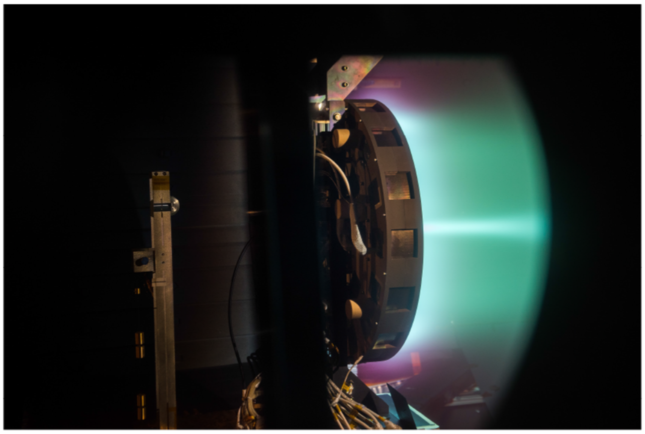

Fig. 2 A photograph of the X3 firing in VF-5.

Each of the X3 NHT's discharge channels can be fired separately or in combination with others, providing seven unique operating configurations. We denote these configurations throughout this paper using "I" for the innermost channel, "M" for the middle channel, and "O" for the outermost channel. For example, the configuration where the inner and middle channels are firing together is denoted as the IM configuration. This was the configuration tested for all points described herein, as the outer channel was not used.

During this test campaign, the thruster was electrically isolated from the thrust stand inside the vacuum facility but then tied to facility ground on the atmosphere side of the test setup with a dedicated body grounding strap. The current collected by the grounded body was then recorded during testing. For the 90 A total discharge current operation described here, the body collected less than 100 mA, due to the dielectric coating covering the exterior surface of the thruster.

B. Vacuum Facility and Test Equipment

The testing described here was performed in Vacuum Facility 5 (VF-5) at NASA Glenn Research Center. VF-5 is a 4.6-m-diam, 18.3-m-long cylindrical vacuum chamber that features 33 m^2 of cryogenic pump surfaces, providing a pumping speed of 700,000 L/s on xenon. The facility walls and cryogenic panels are lined with graphite plates to minimize backsputter during thruster operation. Pressure inside the facility was monitored using a hot-cathode ionization gauge mounted in the exit plane of the thruster approximately 1.5 m from thruster centerline, pointed downstream, per industry best practices [11]. This gauge was calibrated on xenon and was corrected for orientation using techniques by Yim and Burt [12]. Facility base pressure was typically on the order of 1×10^{-7} Torr during this test campaign. Background pressure while firing the thruster for the testing described here was approximately 19 μTorr-Xe.

A schematic of the location of the X3 NHT inside VF-5, as well as the location of the plasma diagnostics package, is shown in Fig. 3, and a photograph of the X3 NHT installed in VF-5 is shown in Fig. 4. We operated the thruster off of a set of laboratory power supplies, which included six separate supplies for the electromagnets, a cathode heater supply, and a cathode keeper supply. For this experiment, only the inner and middle channels were operated, and as such, only their corresponding electromagnets were powered. Each of the discharge channels was operated from a separate high-voltage, high-current power supply. The inner was operated using a set of three 1000 V, 15 A supplies that were connected in a master/slave configuration, and the middle was operated using a 2000 V, 100 A supply. Each discharge channel featured a 100 μF capacitor across the anode and cathode lines. These capacitors isolated the power supplies from the thruster and allowed the thruster to experience high-current transients without extinguishing. Electric propulsion-grade xenon propellant was provided to the thruster via five electropolished stainless steel feed lines. Each line featured a precision flow controller to prescribe the xenon: a 500 sccm controller for the inner channel, a 1000 sccm controller for the middle channel, a 200 sccm controller for the cathode, and a 200 sccm controller for the cathode external injectors. The fifth line featured a 2000 sccm controller for the outer channel, but as noted this was not used during the testing described herein.

We measured thruster telemetry in a breakout box that contained precision shunts, voltage dividers, and isolation amplifiers that allowed for measurement of discharge, magnet, and cathode telemetry. This telemetry was collected by a data logger controlled by LabView. Telemetry was recorded at a rate of approximately 0.3 Hz. In addition to the low-speed measurements taken in the breakout box, high-speed measurements of the discharge currents were taken using a set of clamp-on current sensors read by two oscilloscopes. The discharge current oscillations were characterized using peak-to-peak (P2P) and root-mean-square (RMS) values that were calculated by the oscilloscopes and read by the telemetry data logger.

C. Thrust Stand

We designed and built a new inverted-pendulum thrust stand capable of measuring up to 8 N of thrust for this test campaign. The stand was based heavily on the large-thruster thrust stand developed by Hall previously [4]. The thrust stand operates in null mode, is calibrated in situ using a string of known masses, has active inclination control, and is water-cooled to protect against thermal drift during thruster operation, following industry best practices [13–15]. More detailed

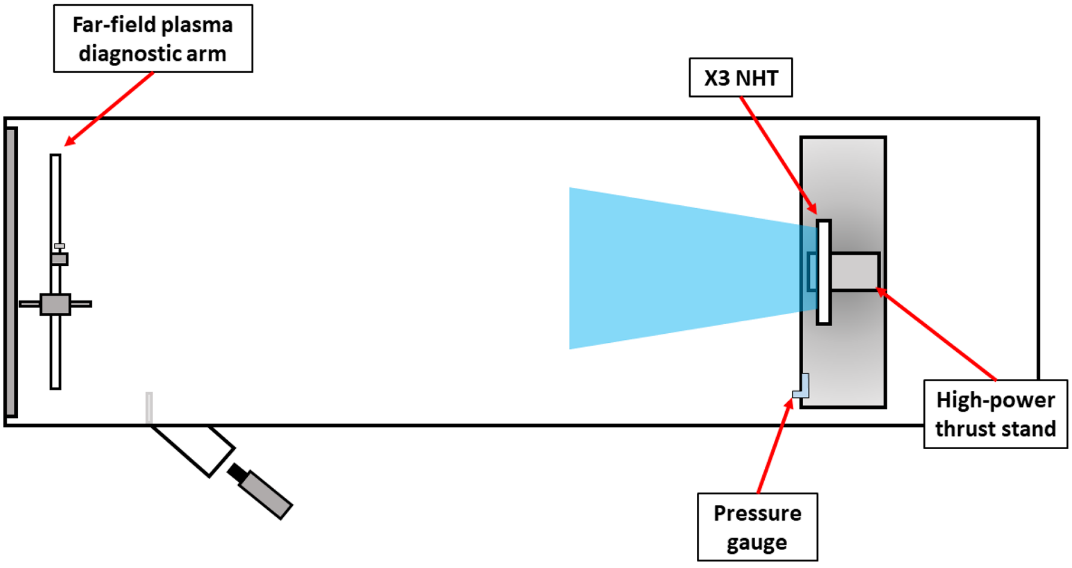

Fig. 3 A schematic showing the location of the X3 as well as diagnostic equipment inside VF-5. Schematic is not to scale.

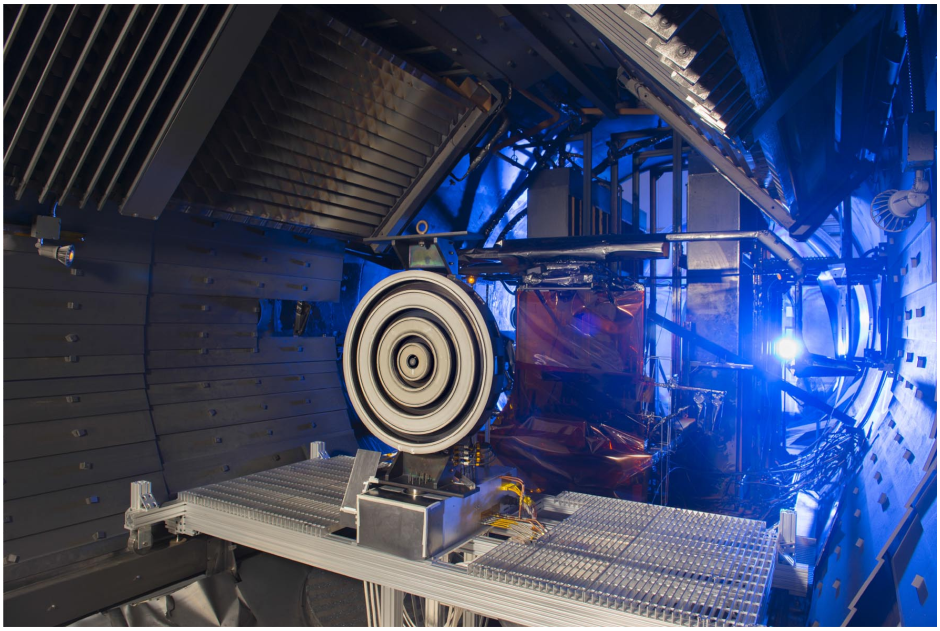

Fig. 4 The X3 NHT installed inside VF-5.

information on the design and operation of the thrust stand is provided by Hall [4].

Based on data collected throughout the test, the thrust stand was found to have a statistical uncertainty of approximately 2%, plus an additional 14 mN uncertainty due to the resolution of the inclination reading. We performed in situ calibrations of the stand at the beginning and end of each test day, and additionally took zeros periodically throughout the day.

D. Langmuir Probe

We used a Langmuir probe (LP) [16] to measure the downstream plasma potential V_p, which is used both in the calculation of acceleration voltage V_{acc} in conjunction with the (RPA) and in the calculation of the coupling voltage Φ_c in accordance with Eq. (6). The LP was a circular planar probe featuring a 3.03 cm^2 molybdenum collector area, which was positioned perpendicular to the beam direction. We swept the LP at 10 Hz from -20 to $+20$ V relative to facility ground in a triangle wave using a function generator driving a bipolar power supply.

We performed data reduction using traditional LP theory [16–18]. Because of the binning process in the LP data analysis method, the uncertainty in V_p was ± 0.5 V at all conditions. This uncertainty contributed ± 0.002 at 300 V discharge voltage to the uncertainty of η_v. This uncertainty combines with that from the RPA to describe the full uncertainty on η_v.

E. Retarding Potential Analyzer

We used an RPA to measure the ion energy distribution function of the plume ions. The RPA is a plasma diagnostic that uses a series of biased and swept grids to selectively collect ions of a certain energy [17]. The RPA used in this experiment featured four grids and a collector: a floating grid at the entrance, an electron repelling grid that was biased to 30 V below ground, the ion selector grid that we swept from 0 to 600 V (twice the thruster discharge voltage), and the secondary electron emission repression grid that was also biased to 30 V below ground. The RPA was located approximately on thruster centerline. We biased the ion selector grid with a commercially available source meter and measured the collected current with a commercially available picoammeter. The RPA had an opening of 5.1 cm^2, but in an effort to minimize the plasma entering the probe at higher power conditions, this opening was reduced to 0.051 cm^2 using a grafoil shield. The acceptance angle of the RPA in this configuration was large enough that the entire thruster was visible to the probe. Other than this modification to the aperture size, no modifications were made to the design or operation of the RPA for use with a high-power thruster. However, we selected the location of the RPA within the thruster plume such that the expected conditions were similar to the previous uses of the RPA, and far enough downstream of the thruster to avoid thermal concerns.

We performed data reduction of the RPA traces similar to what was described by Huang et al. [19]. First, we smoothed the raw traces using the Savitzky–Golay method [20], and then took a numerical derivative of the collected current I_c with respect to ion selector grid bias V_b. The negative of this derivative $(-dI_c/dV_b)$ is proportional to the ion energy distribution function if one can assume a single ion species [17]. For calculation of the thruster voltage utilization efficiency, the RPA is used to calculate the ion energy per charge. Following Huang et al., average voltage V_{avg} was used in place of the traditional most probable voltage V_{mp} for its robustness against noise. We found in our analysis of data from a much larger experimental campaign on the X3 NHT that average voltage was typically identical to most probable voltage except in cases of excessive noise in the probe trace [4]. All results presented here featured negligible noise, and as such, our reported average voltage can be considered equivalent to most probable voltage.

The bias applied to the ion selection grid in the RPA was with respect to ground. However, the voltage through which ions are accelerated out of the thruster is with respect to the far-field plasma potential. Thus, the V_{avg} value was corrected by

$$V_{\mathrm{acc}} = V_{\mathrm{avg}} - V_p \tag{9}$$

where V_{acc} is the acceleration voltage and V_p is the plasma potential, which was measured using the LP described above. We then used acceleration voltage V_{acc} to calculate voltage utilization efficiency as defined in Eq. (7).

We found an average uncertainty on V_{avg} of ± 1.04 V for our analysis technique. This average uncertainty corresponds to an average uncertainty in η_v of ± 0.003 at 300 V discharge voltage. This brings the total uncertainty on η_v to ± 0.015 for the operating conditions described here.

III. Results

During this test campaign we demonstrated for the first time operation of the X3 NHT at reduced cathode flow fractions. For the IM condition at 300 V and 27.2 kW total discharge power (26.3 A on the inner channel and 64.2 A on the middle), we reduced the TCFF from 7 to 3% in 1% increments, leaving $\dot{m}_c$ at the nominal 16 sccm

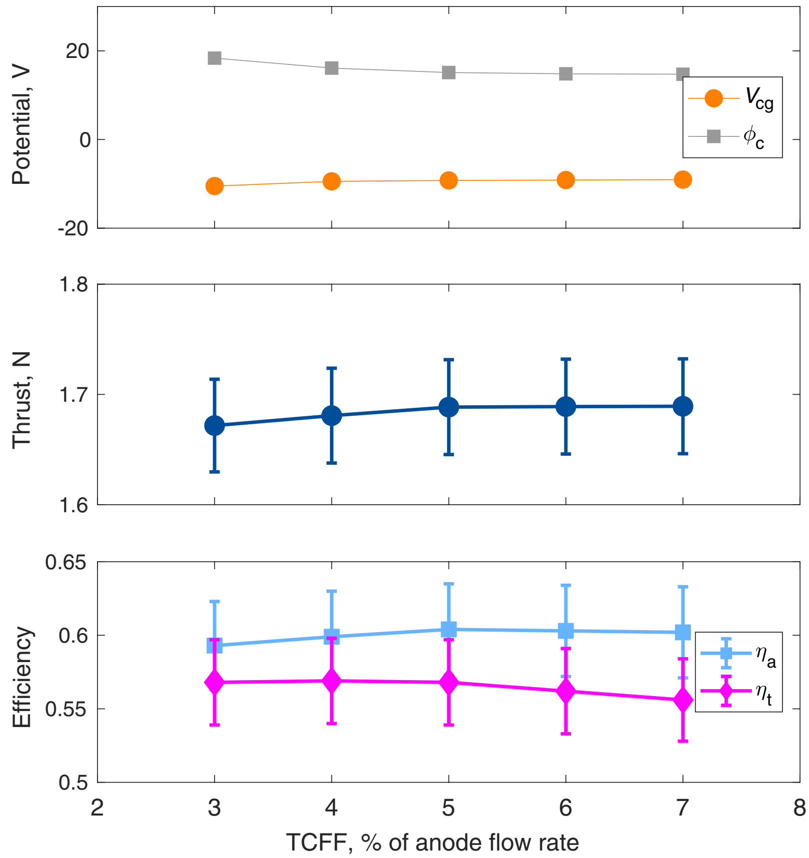

Fig. 5 Thruster performance parameters plotted as a function of total cathode flow fraction.

and reducing $\dot{m}_{inj}$. At each TCFF setting, we measured thruster performance with the thrust stand as well as the acceleration voltage and plasma potential using the downstream plasma diagnostics package. This range of TCFF values was selected to encompass the nominal value used during high-power thruster characterization at 7% and to decrease just beyond the recommended minimum flow rate for the cathode as identified during cathode development at 3% [4,7].

Figure 5 shows the trends of the cathode to ground voltage, coupling potential, thrust, anode efficiency, and total efficiency as a function of TCFF. We found that cathode to ground voltage only moved 1.5 V more negative in going from 7% TCFF to 3% TCFF. As the figure shows, over 1 V of this decrease occurred between 4 and 3% TCFF. It is worth noting that 3% TCFF for this thruster operating condition resulted in an injector flow rate below the recommended 20 sccm minimum found during standalone cathode testing [9]. It can be seen that coupling voltage increases with decreasing TCFF. This increase comes both from a decrease in cathode to ground voltage and an increase in plasma potential.

Thrust decreased approximately 17 mN in going from 7% TCFF to 3% TCFF, which corresponds to 1% of the thrust value. Approximately half of this drop occurred in going from 7 to 4%, and the remainder occurred in going from 4 to 3%, which corresponded to the 1 V drop more negative in cathode to ground voltage. Thrust uncertainty at this test point was approximately ±43 mN, corresponding to 2.6% of full scale. Thus, the recorded decrease in thrust across the full range of TCFFs tested was within the uncertainty of the measurement.

We found that anode efficiency increased slightly between 7 and 5% TCFF before decreasing from 5 to 3% TCFF. Anode efficiency values fell within a range of approximately 0.01. Because of the thrust uncertainty, the anode efficiency value had an uncertainty of ±0.03, so these changes fell within the uncertainty of the measurements. Finally, total efficiency increased 0.013 in going from 7 to 3% TCFF. This demonstrates that the efficiency gains from the lower cathode propellant flow rates overcame the inefficiencies imposed on the thruster discharge due to these lower flow rates.

Voltage utilization efficiency as a function of TCFF is presented in Fig. 6. We found that, much like the other parameters, η_V held nearly constant for TCFFs from 7 to 4% at approximately 0.93 before experiencing a drop of nearly 0.03 in going from 4% TCFF to 3%.

We collected high-speed measurements of the discharge current using the current sensors and oscilloscopes described above. These measurements indicate whether dropping the cathode flow fraction has induced a mode transition in the thruster. Figure 7 plots the P2P value of the discharge current oscillations for each channel as a fraction of the mean discharge current of that channel against TCFF. As can be seen, the oscillation amplitudes of both channels decrease

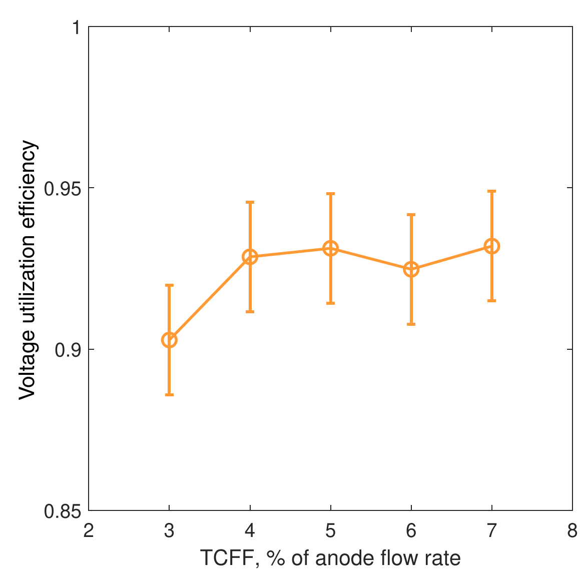

Fig. 6 Voltage utilization efficiency as a function of total cathode flow fraction.

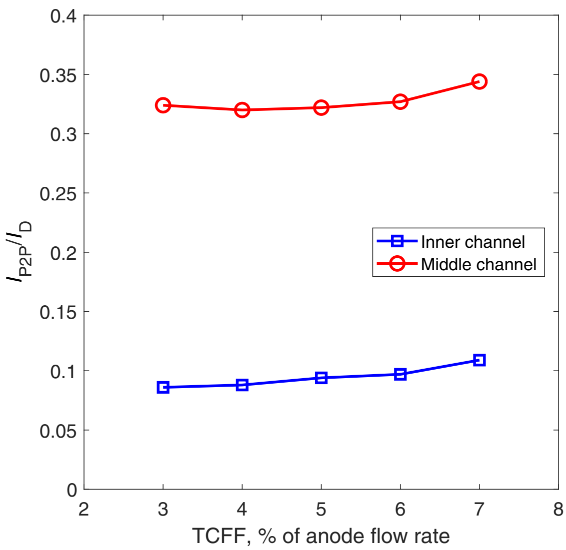

Fig. 7 Normalized discharge current oscillations as a function of total cathode flow fraction.

slightly with decreasing TCFF, but stay constant to within 0.02 throughout the sweep. Mode transitions in Hall thrusters are typically accompanied by large changes in oscillation amplitude [21–23]. Thus, these results indicate that the mode of operation of both channels remained constant during the TCFF sweep.

IV. Discussion

Hall thruster cathode coupling is an area of active research, and the specific physical processes and underlying mechanisms are still poorly understood [24–26]. The topic is of interest not only for thruster/cathode system optimization but also for understanding of the effects that the test environment has on thruster operation. Research into these so-called facility effects has demonstrated repeatedly that cathode coupling, as characterized through the cathode coupling potential, is enhanced (smaller cathode coupling potential) as facility background pressure, and thus neutral density, increases. Additional recent work has shown that the neutral density in the near-cathode region influences both the operation of the cathode itself [7,27] and its coupling to the Hall thruster discharge [28]. Specifically, Jorns et al. showed that increased neutral density in the near-field cathode plume contributes to enhanced collisionality through both classical and nonclassical mechanisms [28]. It is suspected that this result explains the trends seen in facility effect studies, though more work is needed to confirm this.

Thus, though research continues on the subject, it is clear that we can study the neutral density in the near-field cathode region to offer insight into the cathode coupling in the X3 NHT. Because the X3 NHT's cathode features downstream neutral injectors, and because the flow rate through these injectors was what we varied in this experiment (not flow through the cathode center), we can reasonably assume that the ionization fraction of the cathode plume was not strongly dependent on changes in TCFF as tested here. Thus, TCFF offers a reasonable proxy for near-field neutral density, in lieu of actual density measurements.

In Table 1, we present the flow rate in sccm corresponding to each TCFF value tested here. Alongside those values from this test, we calculate the theoretical flow rate corresponding to each TCFF value

Table 1 Total cathode flow rate in sccm of xenon corresponding to various values of total cathode flow fraction for the IM condition tested alongside theoretical calculations for each channel operating individually

TCFF	3%	4%	5%	6%	7%	8%	9%	10%
Inner (theory)	8	10	13	16	18	21	23	26
Middle (theory)	19	26	32	38	45	51	58	64
Inner + middle (actual)	27	36	44	53	62	— —	— —	— —

for the inner and middle channels each operating individually at the same condition (26.3 A for the inner channel and 64.2 A on the middle channel). This allows us to compare the near-cathode neutral density environment for the IM configuration to that for each channel operating individually. We find that the lowest flow rate tested (a TCFF of 3%, corresponding to 27 sccm) is equivalent to a 10% TCFF for the inner channel operating on its own. The middle channel, because it operates at approximately double the discharge current of the inner and thus approximately double the anode flow, has cathode flow rates that are closer to those required for the IM condition. Still, the results indicate that the near-cathode neutral density for the IM condition operating at 4% TCFF is similar to that at 6% TCFF for the middle channel operating on its own. It is worth noting that cross-channel neutral ingestion is a well-documented phenomenon on NHTs, but this simple analysis does not take this into account [4,5]. Thus, it is likely that the neutral density in front of the cathode for the IM condition is equivalent to even higher single-channel TCFF values because of the extra neutrals being contributed by the multiple operating channels.

Taken together, these calculations demonstrate that the neutral density of the near-cathode plume is higher for the IM condition at a given TCFF than it would be for either channel operating individually, substantially so for the inner channel. This then indicates that the collisionality in the cathode plume is enhanced, likely resulting in enhanced cathode coupling. It is also worth noting that cathode coupling voltage (as shown in Fig. 5a) was relatively insensitive to TCFF except at low values. This then suggests that, as long as a minimum neutral density is established, cathode coupling may be maintained and is not significantly enhanced by further increases in neutral density. These results are consistent with the cathode-only results reported by Goebel for the X3 NHT cathode, wherein the cathode was stably operated to currents up to 250 A into a cylindrical anode at total flow rates (injectors and cathode center) of about 25 sccm. Though the physics of cathode-only operation differ substantially [7] from operation with a Hall thruster, our results here suggest that the optimization of cathode operation performed in a stand-alone configuration may translate favorably to operation in a Hall thruster.

Combined, these results in turn suggest that the cathode flow in a high-power Hall thruster may best be set as the lowest reasonable flow rate to provide the necessary neutral density in the near-plume of the cathode instead of a fixed fraction of anode flow rate. This becomes of increased importance for NHTs, which have a larger throttling range than traditional single-channel thrusters. If the proper neutral environment is created in the near plume of the cathode, one possibly dictated by the cathode design as opposed to the thruster's operating condition, it may be possible to effectively couple across a wide range of throttling points at the same cathode flow rate. This could potentially result in TCFF values significantly below 3% for higher-power operating conditions of the X3 NHT. However, we emphasize that the coupling of multiple Hall thruster discharge channels to a single shared cathode is a poorly understood phenomenon, and our analysis should be taken as a first step toward understanding the problem.

V. Conclusions

This test demonstrated that the X3 NHT can be operated stably at TCFFs of as low as 4% without significant impact on thruster operation. In fact, due to the reduced flow rates, the total efficiency is slightly increased (although all values are within the measurement uncertainty). Even at as low as 3% TCFF, the decrease in thruster performance remains within the measurement uncertainty and the thruster exhibits no increase in discharge current oscillations. These results suggest that low-TCFF operation is feasible for high-power Hall thrusters and can offer increased system efficiency as well as improved cathode lifetime, and can do so with little impact on thruster operation. This makes low-TCFF operation of interest from a system development perspective, for instance, for the development of the XR-100 system that incorporates the X3 NHT and the high-current cathode [29].

As an illustration of the potential impact on mission design from low-TCFF operation, consider a system operating at 250 A discharge current. A reduction in TCFF from 10 to 4% corresponds to a savings of approximately 15 mg/s of xenon. For an example thruster lifetime of 10 kh, this corresponds to a savings of 540 kg of xenon propellant.

However promising these initial results are, further work is necessary to verify these trends with other X3 NHT channel combinations and operating points. There are many questions left unanswered by this test, including many related to the physics and operation of NHTs in general. Anecdotal experiences while operating the X3 led us to the conclusion that a higher TCFF is likely necessary during changes in thruster operating condition. For instance, that while operating at 5% TCFF in the MO configuration, the inner channel ignited with discharge oscillations in excess of 110%. Increasing the TCFF to 7% reduced these oscillations to nominal values. Higher TCFF, especially on this cathode, where this translates to more cold neutral gas being deposited at the exit of the cathode, quenches oscillations and improves the cathode coupling to the anodes. The shock of lighting a new channel may cause issues with that anode coupling to the cathode that is already coupled to as many as two other channels. However, once the coupling is established between the new channel and the cathode, it is possible that the TCFF could again be decreased without issue. These types of phenomena are very poorly understood in NHTs and represent some of the research that remains with these devices [4].

Long-term thruster stability at low TCFF was also not studied here. The test described here consisted of operation at each TCFF value of less than 15 minutes, and during the entire test the thruster experienced no major discharge transients. It is possible that at low TCFF a spark event or other momentary change in thruster behavior could destabilize the thruster discharge for one or more channels. These questions are a subset of broader questions being answered by the community at large. Understanding in more detail the sources of Hall thruster discharge oscillations and the role that ground-test facilities play in the phenomena observed during thruster operation will provide further insight into questions of cathode coupling and low-TCFF operation.

Acknowledgments

At the time of this work, Scott J. Hall was supported by a NASA Space Technology Research Fellowship under grant number NNX14AL67H. A portion of the work described here was performed as a part of NASA's NextSTEP program under grant number NNH16CP17C. The plasma diagnostics in this experiment were funded by a Michigan Institute of Plasma Science and Engineering Graduate Student Fellowship. A portion of this work was carried out at the Jet Propulsion Laboratory, California Institute of Technology, under a contract with NASA. The authors gratefully acknowledge Joshua M. Woods of the University of Michigan for assistance with the plasma diagnostics. The authors would like to acknowledge a number of personnel at NASA Glenn Research Center who contributed to this work, including Hani Kamhawi, Peter Y. Peterson, James E. Gilland, Eric Pencil, Luis Piñero, Chad Joppeck, Taylor Varouh, Nick Lalli, Richard Senyitko, Jim Zakany, Jim Szelogowski, Kevin Blake, Josh Gibson, Larry Hambly, George Jacynycz, and Dave Yendriga.

References

[1] Goebel, D., Jameson, K. K., and Hofer, R. R., "Hall Thruster Cathode Flow Impact on Coupling Voltage and Cathode Life," *Journal of Propulsion and Power*, Vol. 28, No. 2, 2012, pp. 355–363. https://doi.org/10.2514/1.B34275

[2] Manzella, D., "Scaling Hall Thrusters to High Power," Ph.D. Thesis, Stanford Univ., Stanford, CA, 2005.

[3] Hall, S. J., Jorns, B. A., Gallimore, A. D., Kamhawi, H., Haag, T. W., Mackey, J. A., Gilland, J. H., Peterson, P. Y., and Baird, M. J., "High-Power Performance of a 100-kW Class Nested Hall Thruster," *35th International Electric Propulsion Conference*, Electric Rocket Propulsion Soc. Paper IEPC-2017-228, 2017.

[4] Hall, S. J., "Characterization of a 100-kW Class Nested-Channel Hall Thruster," Ph.D. Thesis, Univ. of Michigan, Ann Arbor, MI, 2018.

[5] Liang, R., "The Combination of Two Concentric Discharge Channels into a Nested Hall-Effect Thruster," Ph.D. Thesis, Univ. of Michigan, Ann Arbor, MI, 2013, http://hdl.handle.net/2027.42/100043.

[6] Peterson, P. Y., Jacobson, D. T., Manzella, D. H., and John, J. W., "The Performance and Wear Characterization of a High-Power High-Isp NASA Hall Thruster," *41st AIAA/SAE/ASEE Joint Propulsion Conference*, AIAA Paper 2005-4243, 2005. https://doi.org/10.2514/6.2005-4243

[7] Goebel, D. M., and Chu, E., "High-Current Lanthanum Hexaboride Hollow Cathode for High-Power Hall Thrusters," *Journal of Propulsion and Power*, Vol. 30, No. 1, 2014, pp. 35–40. https://doi.org/10.2514/1.B34870

[8] Goebel, D. M., and Katz, I., *Fundamentals of Electric Propulsion: Ion and Hall Thrusters*, Wiley, Hoboken, NJ, 2008, Chap. 6.

[9] Chu, E., Goebel, D. M., and Wirz, R. E., "Reduction of Energetic Ion Production in Hollow Cathodes by External Gas Injection," *Journal of Propulsion and Power*, Vol. 29, No. 5, 2013, pp. 1155–1163. https://doi.org/10.2514/1.B34799

[10] Florenz, R. E., "The X3 100-kW Class Nested-Channel Hall Thruster: Motivation, Implementation, and Initial Performance," Ph.D. Thesis, Univ. of Michigan, Ann Arbor, MI, 2013.

[11] Dankanich, J. W., Walker, M., Swiatek, M. W., and Yim, J. T., "Recommended Practice for Pressure Measurement and Calculation of Effective Pumping Speed in Electric Propulsion Testing," *Journal of Propulsion and Power*, Vol. 33, No. 3, 2017, pp. 668–680. https://doi.org/10.2514/1.B35478

[12] Yim, J., and Burt, J. M., "Characterization of Vacuum Facility Background Gas Through Simulation and Considerations for Electric Propulsion Ground Testing," *51st AIAA/SAE/ASEE Joint Propulsion Conference*, AIAA Paper 2015-3825, 2015. https://doi.org/10.2514/6.2015-3825

[13] Haag, T., "Thrust Stand for High-Powered Electric Propulsion Devices," *Review of Scientific Instruments*, Vol. 62, No. 5, 1991, pp. 1186–1191. https://doi.org/10.1063/1.1141998

[14] Xu, K. G., and Walker, M. L., "High-Power, Null-Type, Inverted Pendulum Thrust Stand," *Review of Scientific Instruments*, Vol. 80, No. 5, 2009, Paper 055103. https://doi.org/10.1063/1.3125626

[15] Polk, J. E., Pancotti, A., Haag, T., King, S., Walker, M., Blakely, J., and Ziemer, J., "Recommended Practice for Thrust Measurement in Electric Propulsion Testing," *Journal of Propulsion and Power*, Vol. 33, No. 3, 2017, pp. 539–555. https://doi.org/10.2514/1.B35564

[16] Lobbia, R. B., and Beal, B. E., "Recommended Practice for Use of Langmuir Probes in Electric Propulsion Testing," *Journal of Propulsion and Power*, Vol. 33, No. 3, 2017, pp. 566–581. https://doi.org/10.2514/1.B35531

[17] Hutchinson, I. H., *Principles of Plasma Diagnostics*, 2nd ed., Cambridge Univ. Press, New York, 2002, Chap. 3.

[18] Lieberman, M. A., and Lichtenberg, A. J., *Principles of Plasma Discharges and Materials Processing*, 2nd ed., Wiley, Hoboken, NJ, 2005, Chap. 6.

[19] Huang, W., Shastry, R., Soulas, G. C., and Kamhawi, H., "Farfield Plume Measurement and Analysis on the NASA-300M and NASA-300MS," *33rd International Electric Propulsion Conference*, Electric Rocket Propulsion Soc. Paper IEPC-2013-057, 2013.

[20] Savitzky, A., and Golay, M. J., "Smoothing and Differentiation of Data by Simplified Least Squares Procedures," *Analytical Chemistry*, Vol. 36, No. 8, 1964, pp. 1627–1639. https://doi.org/10.1021/ac60214a047

[21] Brown, D. L., "Investigation of Low Discharge Voltage Hall Thruster Characteristics and Evaluation of Loss Mechanisms," Ph.D. Thesis, Univ. of Michigan, Ann Arbor, MI, 2009.

[22] Hara, K., Sekerak, M. J., Boyd, I. D., and Gallimore, A. D., "Mode Transition of a Hall Thruster Discharge Plasma," *Journal of Applied Physics*, Vol. 115, No. 20, 2014, Paper 203304. https://doi.org/10.1063/1.4879896

[23] Sekerak, M. J., Gallimore, A. D., Brown, D. L., Hofer, R. R., and Polk, J. E., "Mode Transitions in Hall-Effect Thrusters Induced by Variable Magnetic Field Strength," *Journal of Propulsion and Power*, Vol. 32, No. 4, 2016, pp. 903–917. https://doi.org/10.2514/1.B35709

[24] Beal, B. E., Gallimore, A. D., and Hargus, W. A., "Effects of Cathode Configuration on Hall Thruster Cluster Plume Properties," *Journal of Propulsion and Power*, Vol. 23, No. 4, 2007, pp. 836–844. https://doi.org/10.2514/1.24636

[25] Sommerville, J. D., and King, L. B., "Hall-Effect Thruster–Cathode Coupling, Part I: Efficiency Improvements from an Extended Outer Pole," *Journal of Propulsion and Power*, Vol. 27, No. 4, 2011, pp. 744–753. https://doi.org/10.2514/1.50123

[26] Sommerville, J. D., and King, L. B., "Hall-Effect Thruster–Cathode Coupling, Part II: Ion Beam and Near-Field Plume," *Journal of*

Propulsion and Power, Vol. 27, No. 4, 2011, pp. 754–767. https://doi.org/10.2514/1.50124

[27] Mikellides, I., Ortega, A. L., Goebel, D. M., and Becatti, G., "Dynamics of a Hollow Cathode Discharge in the Frequency Range of 1–500 kHz," *Plasma Sources Science and Technology*, Vol. 29, No. 3, 2020, Paper 035003. https://doi.org/10.1088/1361-6595

[28] Jorns, B. A., Cusson, S. E., Brown, Z., and Dale, E., "Non-Classical Electron Transport in the Cathode Plume of a Hall Effect Thruster," *Physics of Plasmas*, Vol. 27, No. 2, 2020, Paper 022311. https://doi.org/10.1063/1.5130680

[29] Shark, S. W., Hall, S. J., Jorns, B., Hofer, R. R., and Goebel, D. M., "High Power Demonstration of a 100 kW Nested Hall Thruster System," *2019 AIAA Propulsion and Energy Forum*, AIAA Paper 2019-3809, 2019. https://doi.org/10.2514/6.2019-3809

J. Blandino
Associate Editor